Protein Science (1994), *3*:64–69. Cambridge University Press. Printed in the USA.

Crystal structure of the unactivated ribulose 1,5-bisphosphate carboxylase/oxygenase complexed with a transition state analog, 2-carboxy-D-arabinitol 1,5-bisphosphate

KAM Y.J. ZHANG, DUILIO CASCIO, AND DAVID EISENBERG

Molecular Biology Institute and Department of Chemistry and Biochemistry, University of California, Los Angeles, California 90024-1570

(RECEIVED June 10, 1993; ACCEPTED October 5, 1993)

Abstract

The crystal structure of unactivated ribulose 1,5-bisphosphate carboxylase/oxygenase from *Nicotiana tabacum* complexed with a transition state analog, 2-carboxy-D-arabinitol 1,5-bisphosphate, was determined to 2.7 Å resolution by X-ray crystallography. The transition state analog binds at the active site in an extended conformation. As compared to the binding of the same analog in the activated enzyme, the analog binds in a reverse orientation. The active site Lys 201 is within hydrogen bonding distance of the carboxyl oxygen of the analog. Loop 6 (residues 330–339) remains open and flexible upon binding of the analog in the unactivated enzyme, in contrast to the closed and ordered loop 6 in the activated enzyme complex. The transition state analog is exposed to solvent due to the open conformation of loop 6.

Keywords: CABP; photosynthesis; protein crystallography; rubisco

Ribulose 1,5-bisphosphate carboxylase/oxygenase (rubisco, EC 4.1.1.39) is a bifunctional enzyme that catalyzes the initial reactions of two important but competing physiological pathways in green plants: photosynthetic carbon fixation and photorespiration. The Calvin cycle of photosynthetic carbon fixation, initiated by the rubisco-catalyzed carboxylation of ribulose 1,5-bisphosphate (RuBP), is the only significant incorporation of atmospheric carbon into the biosphere (Brändén et al., 1991). In photosynthesis, green plants use chemical energy trapped by light-energized reactions to drive the rubisco-catalyzed fixation of carbon dioxide. But the competing pathway of photorespiration, catalyzed also by rubisco, consumes chemical energy and releases CO_2 into the atmosphere. Photorespiration significantly reduces the net efficiency of photosynthesis and limits crop yields. Rubisco, being an abundant yet inefficient enzyme with a central role in the carbon metabolism of plants, is a prime target in attempts to use protein engineering to increase the yields of agriculturally important crops (Ellis, 1979; Andrews & Lorimer, 1987).

Rubisco must be activated in order to carry out its carboxylation and oxygenation functions (Lorimer et al., 1976). The activation involves the formation of a carbamate between the ϵ-amino group of a conserved lysine (Lys 201 in tobacco) with a nonsubstrate CO_2, known as an activator. This carbamate is stabilized by a metal ion (usually Mg^{2+}) (Lorimer, 1981). Although rubisco is catalytically competent only when it forms a ternary complex of rubisco–CO_2–Me^{2+} (Lorimer et al., 1976; Pierce et al., 1980; Lorimer, 1981), the unactivated rubisco can catalyze the decarboxylation of the transition state intermediate, 2-carboxy-keto-D-arabinitol 1,5-bisphosphate (Pierce et al., 1986). This is the only known catalytic function of the unactivated enzyme.

The atomic structures of rubisco from various sources were solved by X-ray crystallography (for a review, see Brändén et al., 1991). The rubisco from the photosynthetic bacterium *Rhodospirillum rubrum* is a dimer of 2 large subunits (Schneider et al., 1986). However, rubisco from plants and most other photosynthetic organisms is a complex of 8 large and 8 small subunits (Chapman et al., 1986, 1987, 1988; Andersson et al., 1989). The active site is formed between the interface of the C-terminal β/α-barrel domain of a large subunit and the N-terminal domain of a dimer-related large subunit.

We report here the crystal structure of the unactivated rubisco from tobacco complexed with a transition state analog, 2-carboxy-D-arabinitol 1,5-bisphosphate (CABP), refined at 2.7 Å resolution. The mode of binding of CABP, its interaction with residues in the active site, and a comparison with the same analog in activated rubisco are presented.

Reprint requests to: David Eisenberg, Molecular Biology Institute, University of California, Los Angeles, 405 Hilgard Avenue, Los Angeles, California 90024-1570.

Results

The overall structure of the complex of unactivated rubisco with the transition state analog CABP is very similar to that of the unactivated rubisco (Curmi et al., 1992), having an RMS deviation of 0.85 Å for all the nonhydrogen atoms. A superposition of Cα atoms between the unactivated rubisco structures with and without CABP bound is shown in Kinemage 1. The active site residues are little affected by the binding of CABP. A movement of loop 6 (residues 330–339) from open, disordered to close, ordered conformation was observed from the structures of unactivated rubisco (Curmi et al., 1992) and activated rubisco (Schreuder et al., 1993). A similar loop movement during catalysis is also observed in the active site of the crystal structures of triose phosphate isomerase (Alber et al., 1981). In this structure of unactivated rubisco, loop 6 remains flexible upon binding of CABP, as judged by its high temperature factors, which are comparable to those in the structure of unactivated rubisco. Residues in loop 6 make a few hydrogen bonds and hydrophobic interactions with residues of symmetry-related molecules.

A portion of the $2F_o - F_c$ map around CABP (Fig. 1) shows that the carboxyl and hydroxyl groups of the CABP are clearly visible and the residues in the active site are well defined.

The CABP binds across the C-terminal side of the β/α-barrel, in the active site of rubisco, through a network of hydrogen bonds and salt links, as shown in Figure 2. The phosphate groups of the CABP occupy the same position as that of the free sulfate/phosphate in the unactivated rubisco (Curmi et al., 1992). The P1 phosphate is about 0.60 Å away from the free sulfate/phosphate, and the P2 phosphate is about 0.58 Å away from the free sulfate/phosphate, as shown in Figure 3. As judged by the atomic separations of less than 3.8 Å, the P1 phosphate interacts with the side chains of Arg 295, His 298, and Ser 379 in loops 5 and 6 (the numbering scheme is the same as that of Curmi et al., 1992). The P2 phosphate binds to the side chain of Lys 175 and the amide hydrogen of Gly 380, Gly 381, Gly 403, and Gly 404 in loops 1 and 8 at the opposite side of the β/α-barrel. Kinemage 2 shows the mode of binding of CABP in the active site and the corresponding residues in the unactivated rubisco without CABP bound.

When compared to the CABP in the activated rubisco (Schreuder et al., 1993) as explained in the Materials and methods, the CABP binds in the unactivated rubisco in a reverse orientation, as shown in Figure 4 and in Kinemage 3. The reverse mode of binding of CABP is also observed in the structure of inactive rubisco from *R. rubrum* complexed with CABP (Lundqvist & Schneider, 1989). The CABP is more extended in the unactivated than in the activated enzyme. The distance between the 2 phosphate groups of CABP in the unactivated enzyme is 9.72 Å, whereas the distance between the 2 phosphate groups of CABP in the activated enzyme is 8.80 Å. Because of the reversal, the positions of P1 and P2 phosphate groups of CABP are exchanged between the unactivated and activated rubisco. The spatial difference between the P1 in unactivated and P2 in activated rubisco is 1.23 Å. The distance between the P2 in unactivated and P1 in activated rubisco is 1.97 Å. The C2 carboxyl group of CABP points toward Lys 201 and away from loop 6 in the unactivated form, whereas it points toward loop 6 in the activated rubisco. The position of the C2 carboxyl group is shifted about 1.86 Å axially along the CABP. This places the 2 carboxyl oxygens at very different positions. Most noticeably, the O3 and O4 oxygens form hydrogen bonds with the ε-N of Lys 201, which was carbamylated in the activated rubisco. The distance between ε-N of Lys 201 and O3 of CABP is 3.42 Å. The distance between ε-N of Lys 201 and O4 of CABP is 3.43 Å. The position of the side chain of Lys 201 in the unactivated complex was confirmed by simulated annealing omit maps. Since loop 6 remains in an open conformation upon binding of CABP in the active site, the CABP is exposed to solvent with an accessible surface area of 97 $Å^2$ as compared with 7 $Å^2$ in the activated rubisco (Schreuder et al., 1993).

Discussion

As in the structure of unactivated rubisco (Curmi et al., 1992), the active site residues are held together by a network of hydrogen bonds, salt bridges, and van der Waals interactions. In contrast, the forces that hold the free sulfates/phosphates in the active site are weak. Therefore, the sulfates/phosphates can be

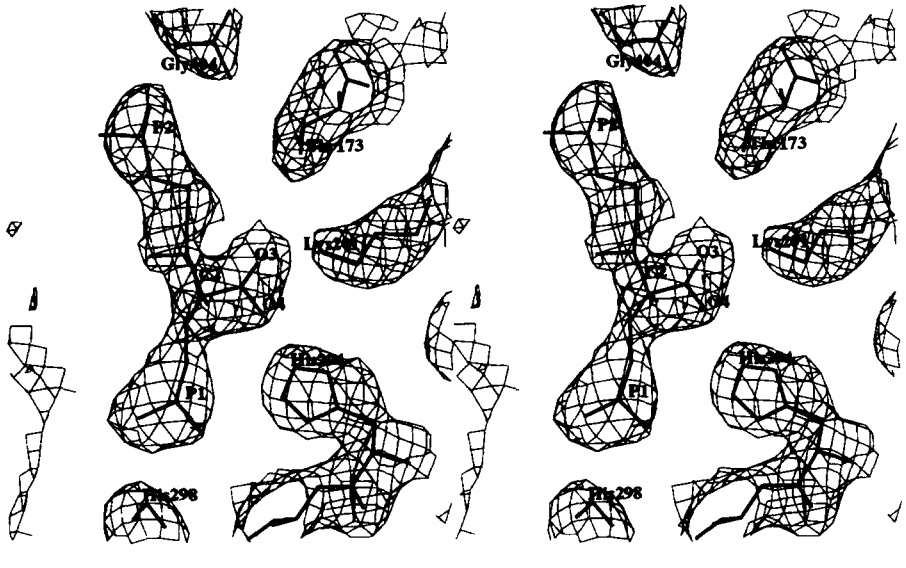

Fig. 1. Stereo pair difference electron density map around the transition state analog CABP, contoured at the 1.0 standard deviation level. The coefficients used are $2F_o - F_c$, where F_o and F_c are the observed and calculated structure factor amplitudes for the binary complex of rubisco with CABP. The phases used are those calculated from the refined model. The refined atomic model (represented by thick solid line) is superimposed. The P1 and P2 phosphates and the C2 carboxyl group are labeled. Those residues in contact with CABP are also marked.

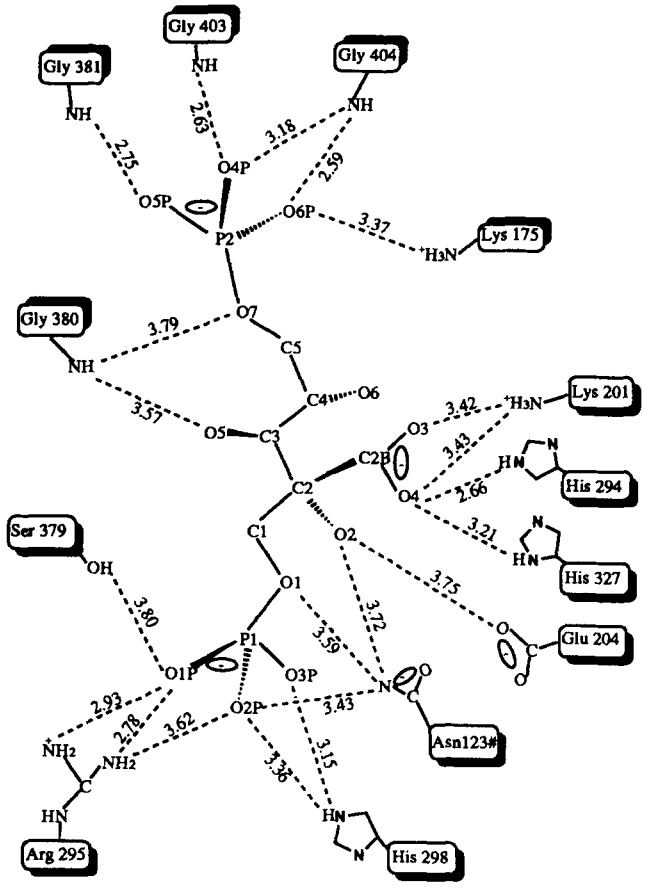

Fig. 2. Schematic diagram showing the polar interactions of CABP with the active site residues of unactivated rubisco. Interacting polar atoms are connected by dashed lines, with distances between them (in Å) indicated. The symbol # indicates residues from symmetry-related molecules.

removed by a desalting process and replaced by CABP, which does not affect the positions of active site residues.

CABP binds in a reverse orientation in unactivated rubisco compared to that in activated rubisco. This suggests that the carbamylation of Lys 201 and the associated metal ion are necessary not only for the activation of rubisco but also for the correct orientation of the substrate. Because the transition state analog in the unactivated rubisco binds in a different orientation than in the activated rubisco, the decarboxylation is not chemically the reverse of the carboxylation step. The decarboxylation can occur with both orientations of substrate, but may be through a different mechanism (Pierce et al., 1986).

Among the residues that interact with CABP, Lys 201 seems to be the most likely candidate to be involved in the decarboxylation of the intermediate. In the binary structure of inactive rubisco from *R. rubrum* with 3-phospho-D-glycerate (3PG), Lundqvist and Schneider (1988) observed that the carboxyl group forms a salt bridge with Lys 191 (equivalent to Lys 201 in tobacco). However, in the complex of inactive rubisco from *R. rubrum* with CABP (Lundqvist & Schneider, 1989), the ϵ-N of Lys 191 is 6.4 Å away from the carboxyl oxygen and thus cannot participate in the decarboxylation reaction. Instead, the data indicated the possible involvement of Asn 111 from a symmetry-related molecule in the decarboxylation. The corresponding residue Asn 123 in this study is not interacting with the carboxyl group of CABP. The nearest atom from Asn 123 to the carboxyl group of CABP is ND2. The distance between ND2 of Asn 123 and O3 of CABP is 4.61 Å. The distance between ND2 of Asn 123 and O4 of CABP is 6.23 Å. The Asn 123 instead interacts with O1, O2, and O2P of CABP, as shown in Figures 2 and 3. There is also biochemical evidence that suggests that Lys 191 in the rubisco from *R. rubrum* is not involved in the decarboxylation (Estelle et al., 1985; Lorimer & Hartman, 1988). However, the structure of unactivated rubisco from tobacco complexed with CABP in our work shows that Lys 201 is within hydrogen bonding distance of the carboxyl oxygen, which might enable Lys 201 to participate in the decarboxylation process.

Comparing the present structure to that of unactivated rubisco (Curmi et al., 1992), there is no significant change observed for loop 6. This suggests that the closure of loop 6 may not be triggered by the binding of substrate but rather by the correct orientation of the substrate. In activated rubisco, the ϵ-N of Lys 334 makes hydrogen bonds with O2 of CABP (3.2 Å distance). However, in unactivated rubisco, O2 is at the opposite side

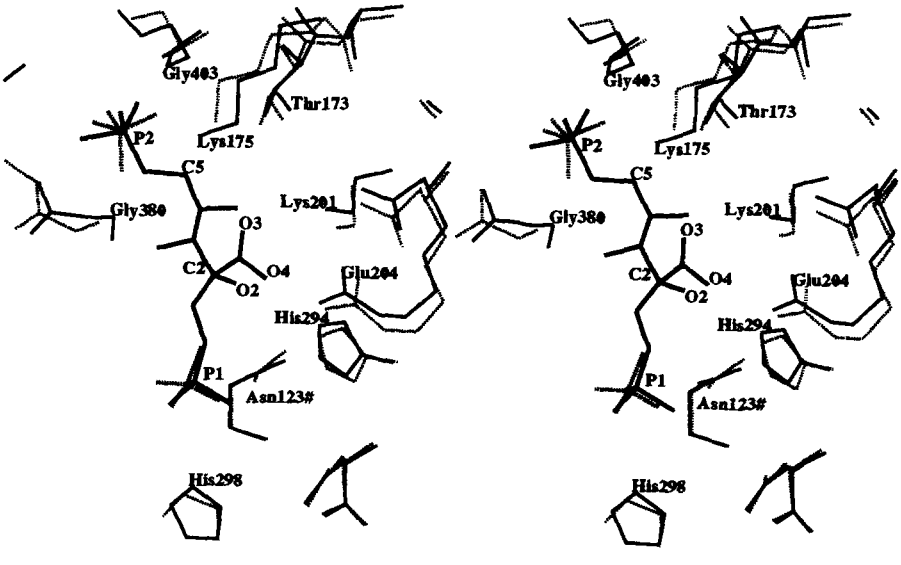

Fig. 3. Stereo view of the active site of unactivated rubisco from tobacco (form III) before and after soaking with CABP. The 2 phosphate groups of CABP, labeled P1 and P2, occupy essentially the same positions as the 2 free sulfates/phosphates found in the unactivated form III rubisco (Curmi et al., 1992). The atomic models of rubisco before and after soaking with CABP are represented by dashed and solid lines, respectively. The CABP model is represented by thick solid lines. Residue Asn 123, marked by #, is from a symmetry-related molecule.

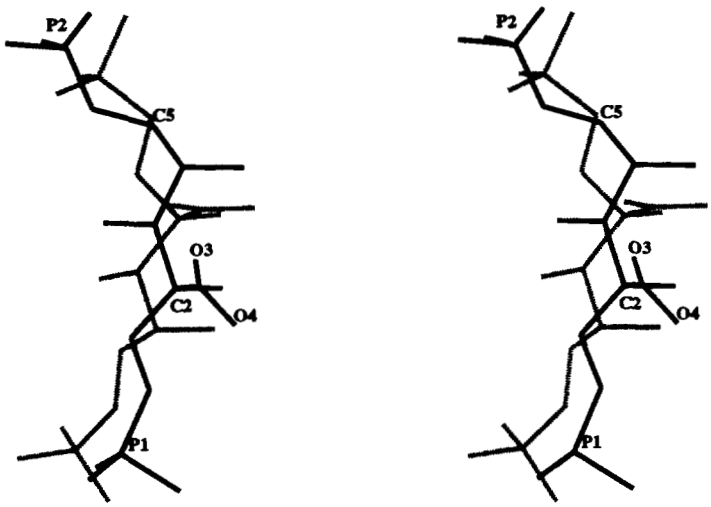

Fig. 4. Stereo view comparison of the orientations of CABP in unactivated (solid line; this work) and activated (broken line; Schreuder et al., 1993) rubisco. The relative orientation of CABP in unactivated and activated rubisco as shown here is the consequence of the superposition of the corresponding protein structures by the algorithm of Kabsch (1978). The CABP in unactivated rubisco is reversed compared to that in activated rubisco. The carboxyl group is not only shifted by 1.86 Å between the CABP in unactivated and activated rubisco but also points in different directions.

of CABP and points away from loop 6, thus making it impossible for Lys 334 to form hydrogen bonds with CABP. Therefore, there is no driving force for the movement of loop 6.

Materials and methods

Purification and crystallization

Rubisco was purified from leaves of *N. tabacum* var. Turkish samsun as described by Chan et al. (1972) and Chapman et al. (1986). Rubisco was stored in 50 mM KH_2PO_4, 0.5 mM EDTA, and 0.5 mM NaN_3 at pH 7.2 with a protein concentration of about 28 mg/mL.

Crystals (form III) were grown according to a modified procedure of Baker et al. (1977) using the hanging drop method. The reservoir contained the precipitant, which is made of 0.2 M KH_2PO_4, 0.3 M $(NH_4)_2SO_4$, and 1 mM NaN_3 at pH 5.2. The hanging drop consisted of between 30 and 70% (v/v) of rubisco solution and precipitant. Large crystals of bipyramidal shape were grown within 1–2 weeks.

Crystal desalting and soaking

The active site of unactivated rubisco is occupied by sulfate/phosphate ions that are used in the crystallization. Orthophosphate and ammonium sulfate were found to be competitive inhibitors with respect to RuBP (Paulsen & Lane, 1966). Therefore, the sulfates/phosphates must be removed before the CABP can be soaked into the active site. A desalting method similar to that of Schreuder et al. (1988; see also Ray et al., 1991) was adopted for the removal of the sulfates/phosphates in the active site. A phosphate- and sulfate-free synthetic mother liquor, made from 20% PEG 8000 (polyethylene glycol 8000), 50 mM NaCl, 1 mM NaN_3, 50 mM MES (2-[*N*-morpholino]ethanesulfonic acid) buffered at pH 5.2, was used. Rubisco form III crystals are stable in this synthetic mother liquor for weeks without losing their diffraction pattern. A form III crystal was transferred into this synthetic mother liquor. This transfer was repeated once per day for a week to ensure the complete removal of sulfates/phosphates. The removal of sulfates/phosphates was confirmed by the difference maps of desalted crystals. Upon completion of the desalting process, 0.2 mM CABP was added to the synthetic mother liquor and the crystal was soaked in this solution for 24 h before data collection.

Data collection

The crystal of rubisco soaked in CABP is in space group I422 with unit cell dimensions of $a = b = 149.0$ Å and $c = 136.8$ Å. A total of 69,151 reflections were collected from 2 crystals using the RAXIS-II imaging plate system with Cu Kα radiation from a Rigaku rotating anode generator. Data collection and processing were carried out by the RAXIS software. The whole data set consists of 19,091 unique reflections, which comprise 92% of all possible reflections, to 2.7 Å resolution with R_{merge} of 9.2% on intensities. A similar data set was also collected for the desalted crystal before soaking in CABP from the same experimental batch, as a control.

Model building and structure refinement

Because the space group and the unit cell of the desalted and soaked crystal did not change significantly, it is assumed that the treated crystal is isomorphous with the original form III crystal. Therefore, the model phases from the unactivated rubisco structure refined at 2.0 Å (Curmi et al., 1992) were used to compute difference maps. The sulfates/phosphates were removed from the model to avoid model bias. We first calculated the difference map shown in Figure 5 using the observed structure factor amplitudes of the desalted crystal and those of the native crystal. This map shows that the sulfates/phosphates were indeed removed. Next, we calculated the difference map between the amplitudes of the desalted and CABP-soaked crystal and that of the model without sulfates/phosphates using the model phases. The map shown in Figure 6 clearly revealed the electron density for CABP bound at the active site. The position of the carboxyl group is well defined. This enabled us to build in the CABP model in an unambiguous orientation. This orientation of the CABP is the reverse of that in the activated rubisco (Schreuder et al., 1993). The rest of the model was taken from the refined structure of unactivated rubisco with slight adjustment of some side chains according to the $2F_o - F_c$ map. The

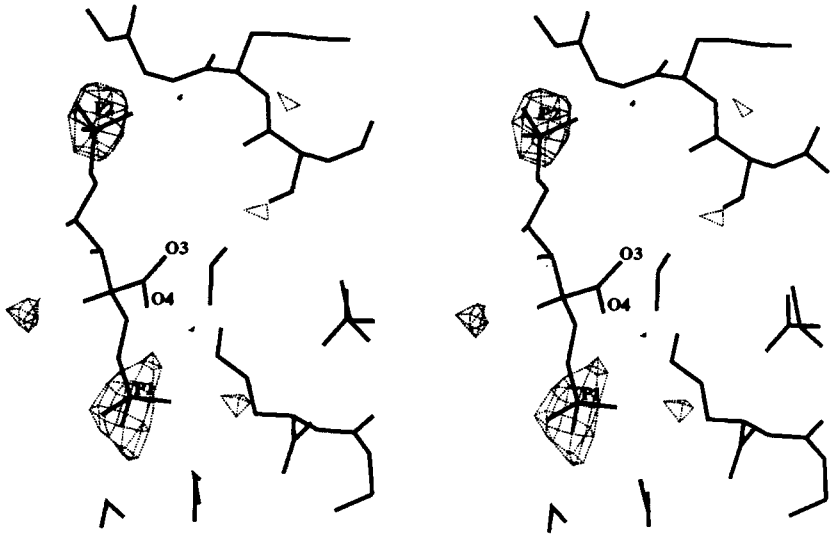

Fig. 5. Difference electron density map at the active site contoured at −3.0 times the standard deviation. The map was calculated with amplitudes $|F_{ods}| - |F_{onat}|$, where F_{ods} and F_{onat} are the observed structure factor amplitudes for the desalted crystal and the native form III crystal, respectively. The phases for the map are calculated from the refined model of the form III rubisco without the 3 free sulfates/phosphates. The initial model of CABP and rubisco is superimposed on the electron density to indicate the positions of the free sulfates/phosphates. The negative density (dashed line) in the difference map shows that the free sulfates/phosphates were removed by the desalting process.

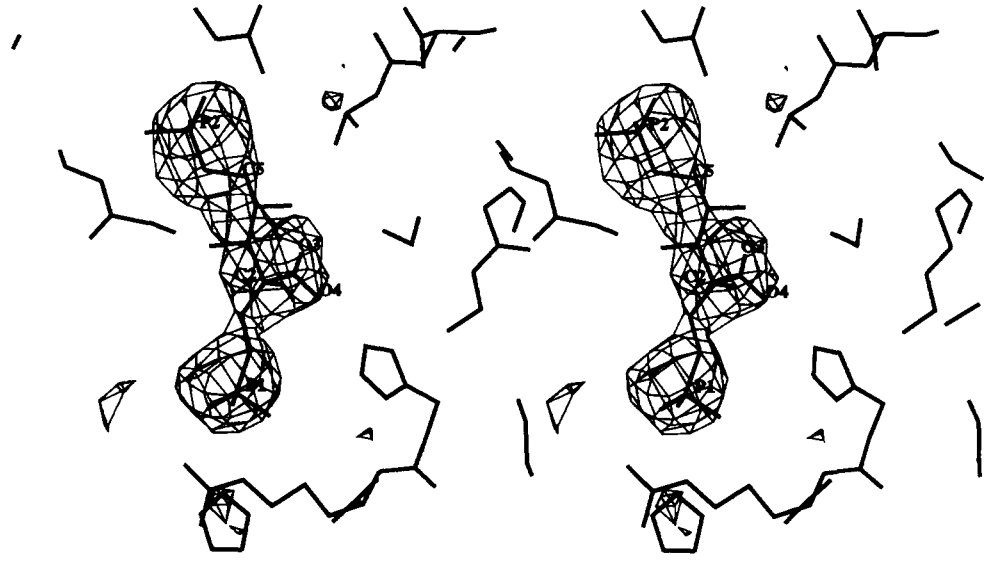

Fig. 6. Difference electron density map at the active site contoured at 3.0 times the standard deviation. The map was calculated with amplitudes $|F_{ocabp}| - |F_{calc}|$, where F_{ocabp} is the observed structure factor amplitude for the desalted crystal soaked with CABP. The F_{calc} and phases are calculated from the refined model of the form III rubisco without the 3 free sulfates/phosphates in the active site. The densities corresponding to the 2 phosphate groups and the carboxyl group of the CABP are strong. This makes the orientation of the CABP unambiguous.

model building was done using FRODO (Jones, 1985). The initial model had an R-factor of 31%. This model was refined by the simulated annealing method using X-PLOR (Brünger, 1990; Brünger et al., 1987). The final model has an R-factor of 19.6% with an RMS deviation of bond length and angle from ideal of 0.018 Å and 3.63 °, respectively. The model has good geometry, as seen from the Ramachandran plot. The Luzzati plot shows that the coordinate error is about 0.25 Å.

Acknowledgments

We thank Dr. Herman Schreuder and Dr. Matthias Wilmanns for helpful discussions. This work was supported by NIH and computer time from the San Diego Supercomputer Center. The coordinates have been deposited with the Protein Data Bank in Brookhaven (PDB code 1RLC).

References

Alber T, Banner DW, Bloomer AC, Petsko GA, Phillips D, Rivers PS, Wilson IA. 1981. On the three-dimensional structure and catalytic mechanism of triose phosphate isomerase. *Philos Trans R Soc Lond B 293*:159–171.

Andersson I, Knight S, Schneider G, Lindqvist Y, Lundqvist T, Brändén CI, Lorimer G. 1989. Crystal structure of the active site of ribulose-bisphosphate carboxylase. *Nature 337*:229–234.

Andrews TJ, Lorimer GH. 1987. Rubisco: Structure, mechanisms, and prospects for improvement. In: Hatch MD, Boardman NK, eds. *The biochemistry of plants, vol 10*. Orlando, Florida: Academic Press. pp 131–218.

Baker TS, Suh SW, Eisenberg D. 1977. Structure of ribulose-1,5-bisphosphate

carboxylase-oxygenase: Form III crystals. *Proc Natl Acad Sci USA 74*:1037–1041.

Brändén CI, Lindqvist Y, Schneider G. 1991. Protein engineering of rubisco. *Acta Crystallogr B 47*:824–835.

Brünger AT. 1990. *X-PLOR version 2.1: A system for crystallography and NMR*. New Haven, Connecticut: Yale University.

Brünger AT, Kuriyan J, Karplus M. 1987. Crystallographic *R* factor refinement by molecular dynamics. *Science 235*:458–460.

Chan PH, Singh KSS, Wildman SG. 1972. Crystalline fraction I protein: Preparation in large yield. *Science 176*:1145–1146.

Chapman MS, Smith WW, Suh SW, Cascio D, Howard A, Hamlin R, Xuong NH, Eisenberg D. 1986. Structural studies of rubisco from tobacco. *Philos Trans R Soc Lond B 313*:367–378.

Chapman MS, Suh SW, Cascio D, Smith WW, Eisenberg D. 1987. Sliding-layer conformational change limited by the quaternary structure of plant rubisco. *Nature 329*:354–356.

Chapman MS, Suh SW, Curmi PMG, Cascio D, Smith WW, Eisenberg D. 1988. Tertiary structure of plant rubisco: Domains and their contacts. *Science 241*:71–74.

Curmi PMG, Cascio D, Sweet RM, Eisenberg D, Schreuder H. 1992. Crystal structure of the unactivated form of ribulose-1,5-bisphosphate carboxylase/oxygenase (rubisco) from tobacco refined at 2.0 Å resolution. *J Biol Chem 267*:16980–16989.

Ellis RJ. 1979. The most abundant protein in the world. *Trends Biochem Sci 4*:241–244.

Estelle M, Hanks J, McIntosh L, Somerville C. 1985. Site-specific Mutagenesis of ribulose-1,5-bisphosphate carboxylase/oxygenase. *J Biol Chem 260*:9523–9526.

Jones TA. 1985. Interactive computer graphics: FRODO. *Methods Enzymol 115*:157–171.

Kabsch W. 1978. A solution for the best rotation to relate two sets of vectors. *Acta Crystallogr A 32*:922–923.

Lorimer GH. 1981. Ribulosebisphosphate carboxylase: Amino acid sequence of a peptide bearing the activator carbon dioxide. *Biochemistry 20*:1236–1240.

Lorimer GH, Badger MR, Andrews TJ. 1976. The activation of ribulose-1,5-bisphosphate carboxylase by carbon dioxide and magnesium ions. Equilibria, kinetics, a suggested mechanism, and physiological implications. *Biochemistry 15*:529–536.

Lorimer GH, Hartman FC. 1988. Evidence supporting lysine 166 of *Rhodospirillum rubrum* ribulosebisphosphate carboxylase as the essential base which initiates catalysis. *J Biol Chem 263*:6468–6471.

Lundqvist T, Schneider G. 1988. Crystal structure of the binary complex of ribulose-1,5-bisphosphate carboxylase/oxygenase and its product, 3-phospho-D-glycerate. *J Biol Chem 263*:3643–3646.

Lundqvist T, Schneider G. 1989. Crystal structure of the complex of ribulose-1,5-bisphosphate carboxylase/oxygenase and a transition state analogue, 2-carboxy-D-arabinitol 1,5-bisphosphate. *J Biol Chem 264*: 7078–7083.

Paulsen JM, Lane MD. 1966. Spinach ribulose diphosphate carboxylase. I. Purification and properties of the enzyme. *Biochemistry 5*:2350–2357.

Pierce J, Andrews TJ, Lorimer GH. 1986. Reaction intermediate partitioning by ribulose-bisphosphate carboxylase with differing substrate specificities. *J Biol Chem 261*:10248–10256.

Pierce J, Tolbert NE, Barker R. 1980. Interaction of ribulose-bisphosphate carboxylase/oxygenase with transition state analogues. *Biochemistry 19*:934–942.

Ray WJ Jr, Bolin JT, Puvathingal JM, Minor W, Liu Y, Muchmore SW. 1991. Removal of salt from a salt-induced protein crystal without cross-linking. Preliminary examination of "desalted" crystals of phosphoglucomutase by X-ray crystallography at low temperature. *Biochemistry 30*:6866–6875.

Schneider G, Lindqvist Y, Brändén CI, Lorimer G. 1986. Three-dimensional structure of ribulose-1,5-bisphosphate carboxylase/oxygenase from *Rhodospirillum rubrum* at 2.9 Å resolution. *EMBO J 5*:3409–3415.

Schreuder HA, Groendijk H, van der Laan JM, Wierenga RK. 1988. The transfer of protein crystals from their original mother liquor to a solution with a completely different precipitant. *J Appl Crystallogr 21*:426–429.

Schreuder HA, Knight S, Curmi PMG, Andersson I, Cascio D, Sweet RM, Brändén CI, Eisenberg D. 1993. Crystal structure of activated tobacco rubisco complexed with the reaction-intermediate analogue 2-carboxyarabinitol 1,5-bisphosphate. *Protein Sci 2*:1136–1146.